

# Finite element formulations of one-dimensional elements with bond-slip

Mohammad R. Salari <sup>a,\*</sup>, Enrico Spacone <sup>b</sup>

<sup>a</sup> *RockSol Consulting Group, Inc., 848 Yellow Pine Ave, Boulder, CO 80304, USA*

<sup>b</sup> *Department of Civil, Environmental and Architectural Engineering, University of Colorado, Boulder, CO 80309-0428, USA*

Received 10 May 2000; received in revised form 18 August 2000; accepted 28 August 2000

## Abstract

This paper presents two general formulations of one-dimensional structural members with deformable interfaces. The interface accounts for the bond-slip between the element components. The first formulation is the classical displacement-based formulation; the second one is a novel force-based approach. The two formulations are derived from the equilibrium and compatibility differential equations of the problem. A special force recovery procedure, based on residual deformations, is presented for the force-based formulation. Two applications are used to illustrate the two formulations: the first is a reinforcing bar with bond slip, the second is a steel–concrete composite beam with partial interaction between the steel beam and the concrete slab. Examples of a bar with bond failure and of a composite beam with weak connection show the precision of the force-based element and its capability to trace the complex response of softening members with a limited number of elements. © 2001 Elsevier Science Ltd. All rights reserved.

*Keywords:* Finite elements; Beam elements; Reinforced concrete beams; Bond-slip; Composite beams; Force-based elements

## 1. Introduction

Recent years have seen the rapid development of force-based formulations for one-dimensional elements, in particular for reinforced concrete members that may show a softening response under axial loads and large lateral deformations. The force-based formulation is particularly attractive for beam elements, since equilibrium can be satisfied exactly along the element, leading to elements that are much more accurate than classical displacement-based elements. The original issue of inserting force-based elements in a general purpose finite element (FE) program has been addressed, among others, by Carol and Murcia [1], Molins and Roca [2], Spacone et al. [3] and Petrangeli and Ciampi [4]. The precision of these elements leads to a drastic reduction in the number of structural degrees of freedom, since in most cases only one frame element per structural member is needed.

Extension of the force-based formulation to one-dimensional members with bond-slip is very important for cases where the partial interaction between different structural components has a significant influence on the overall member response. This is the case, for example, of reinforcing bars with bond-slip, reinforced concrete members with bond slip in the rebars and steel–concrete composite beams. There is widespread experimental evidence that bond-slip plays an important role in increasing the flexibility of reinforced concrete frames, due to bond-slip in the rebars anchored in the foundations or to bond-slip in the beam–column joints. The interaction between steel beam and concrete slab in a composite member is also quite important, especially in determining the effective stiffness of a composite structure. The accurate prediction of the structural stiffness is fundamental in the analysis and design of buildings in seismic active regions. Large differences in the stiffness prediction may lead to gross over or under-estimation of the forces and displacements acting on the structure under the design ground motion.

The main goal of the study presented in this paper was to develop a force-based beam FE for steel–concrete composite beams with partial interaction between the

\* Corresponding author. Tel.: 1-303-998-0697, fax: 1-303-998-0698.

*E-mail address:* salari@rocksol.com (M.R. Salari).

steel beam and the concrete slab. The interaction is due to the slip of the shear studs commonly used in this type of construction. Before developing the composite beam element, the formulation was tested on a simpler bar element with bond-slip. The formulation is identical, but the displacement and deformation fields are much simpler for the bar element.

Starting from the basic differential equations of a one-dimensional element with bond slip (mainly equilibrium and compatibility), this paper presents two general element formulations, the first one displacement-based, the second one force-based. The original element force recovery procedure for force-based elements is presented in detail, together with its extension to the one-dimensional element with bond slip. The formulations are general, and two applications are used to showcase the capabilities of the force-based formulation and to compare it to the displacement-based formulation. One is the problem of a steel rebar with bond-slip, the second is the problem of a steel–concrete beam with partial connection. The applications presented are aimed at showing the precision of the proposed force-based element and its capability of describing complex structural responses with very few elements. From a computational standpoint, the most interesting and challenging of such cases is softening due to bond failure.

## 2. Definitions and problem differential equations

In the present formulations, the deformable body consists of two basic components, namely the main body and the interface. The main body is the principal load-carrying component and is divided into different sub-components by the interface. Only one-dimensional components are considered in this paper. All components are assumed straight and geometric nonlinearities are neglected. Even though the formulations presented hereafter are expressed in general terms, two applications are considered. One is a reinforcing bar with bond-slip, the second is a steel–concrete composite beam with partial interaction between the steel girder and the concrete slab. The steel rebar is shown in Fig. 1. The concrete is modeled as a rigid body, and the interaction between rebar and concrete is lumped in the nonlinear bond-slip constitutive law. The composite beam is illustrated in Fig. 2. The general model includes slab uplift. In the following formulation, however, uplift is neglected, since there is not sufficient experimental evidence supporting the importance of uplift in the response of steel–concrete composite beams.

The displacement field for the steel rebar of Fig. 1 is simply the axial displacement  $\mathbf{u}(x)=u(x)$  of the rebar. The deformation field is the axial strain  $\mathbf{e}(x)=\varepsilon(x)$  and the corresponding force field is the axial load  $\mathbf{s}(x)=N(x)$ . For the composite beam of Fig. 2, the displacement fields

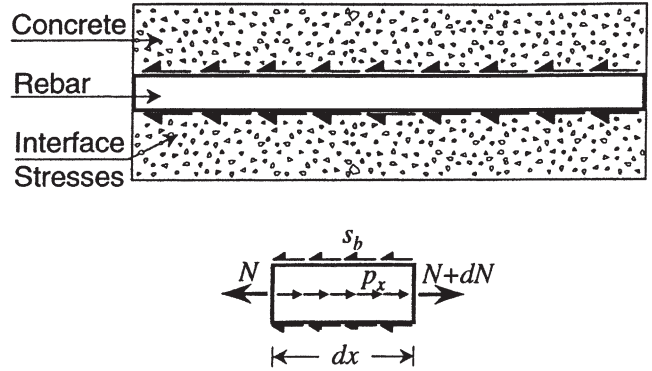


Fig. 1. Reinforcing bar with bond slip: forces on an infinitesimal element.

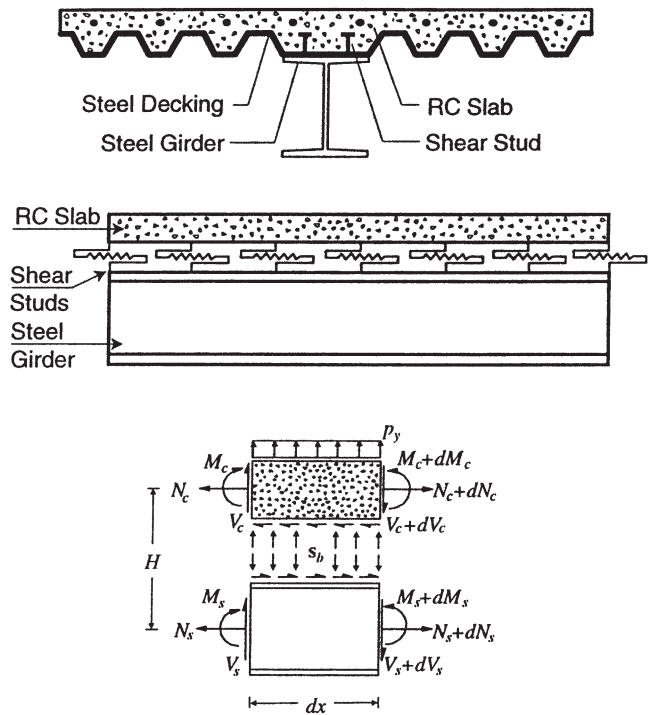


Fig. 2. Composite beam with deformable connection: forces on an infinitesimal element.

are  $\mathbf{u}(x) = \{v(x) \ u_{0c}(x) \ u_{0s}(x)\}^T$ , where  $v(x)$  is the vertical displacement (identical in the beam and in the slab from the assumption of zero uplift),  $u_{0c}(x)$ ,  $u_{0s}(x)$  are the axial displacements of the concrete slab and of the steel beam, respectively, at their reference axes (indicated by subscript 0). The deformation fields are  $\mathbf{e}(x) = \{\kappa(x) \ \varepsilon_{0c}(x) \ \varepsilon_{0s}(x)\}^T$ , where  $\kappa(x)$  represents the curvature and  $\varepsilon_{0c}(x)$ ,  $\varepsilon_{0s}(x)$  are the concrete slab and the steel beam axial strains, respectively. The corresponding force fields are  $\mathbf{s}(x) = \{M(x) \ N_c(x) \ N_s(x)\}^T$ , where  $M(x)$  is the composite section bending moment and  $N_c(x)$ ,  $N_s(x)$  are the concrete slab and the steel beam axial forces, respectively. The element vectors are summarized in Table 1.

Table 1  
Definitions of element vectors for bar with bond slip and for steel–concrete composite beam with partial connection

Vectors	Bar with bond-slip	Composite beam with partial connection
Displacement field	$\mathbf{u}(x)=u(x)$	$\mathbf{u}(x)=\{v(x) u_{0c}(x) u_{0s}(x)\}^T$ (1)*
Section deformations	$\mathbf{e}(x)=\varepsilon(x)$	$\mathbf{e}(x)=\{\kappa(x) \varepsilon_{0c}(x) \varepsilon_{0s}(x)\}^T$ (2)*
Section forces	$\mathbf{s}(x)=N(x)$	$\mathbf{s}(x)=\{M(x) N_c(x) N_s(x)\}^T$ (3)*
Differential operators	$\partial=d/dx$	$\partial=\begin{bmatrix} \frac{d^2}{dx^2} & 0 & 0 \\ 0 & \frac{d}{dx} & 0 \\ 0 & 0 & \frac{d}{dx} \end{bmatrix}$
	$\partial_b=1$	$\partial_b=\begin{bmatrix} \frac{d}{dx} & 1 & -1 \end{bmatrix}$

The differential equations of equilibrium for the deformable body under consideration can be written in the following matrix form

$$\partial^T \mathbf{s}(x) - \partial_b^T \mathbf{s}_b(x) - \mathbf{p}(x) = 0 \quad (1)$$

where  $\partial$ ,  $\partial_b$  are derivative operators defined in Table 1,  $\mathbf{s}_b(x)$  is the generalized interface force vector, and  $\mathbf{p}(x)$  is the body force vector.

Under small displacements, the compatibility conditions can be written as follows

$$\mathbf{e}(x) = \partial \mathbf{u}(x) \quad \mathbf{e}_b(x) = \partial_b \mathbf{u}(x) \quad (2)$$

where  $\mathbf{e}_b(x)$  is the bond-slip (or the relative displacement) at the interface. The above differential equations form the basis of the two FE formulations presented in the following section.

### 3. Finite element formulations

Two distinct FE formulations are presented hereafter for modeling the behavior of one dimensional elements with bond-slip. A classical displacement-based formulation is briefly described first, followed by the presentation of a force-based formulation. The formulations are first discussed in a general format. Applications to the bar with bond slip and to the composite beam with partial connection are presented later in the paper. In the following formulations, dependency of section forces and deformations on  $x$  is omitted in order to simplify the notation. In addition, the body forces  $\mathbf{p}(x)$  are omitted since they are not central to the formulations.

#### 3.1. Displacement-based element

In a displacement-based FE formulation, the element displacements are expressed in terms of the element nodal displacements through appropriate displacement

interpolation functions. Section deformations are obtained by enforcing the compatibility conditions of (2). Compatibility is thus satisfied in a strict sense along the element. By applying the force–deformation relations at any section, section forces can be obtained. Section forces must satisfy the equilibrium conditions in (1). To enforce these conditions at the current element state, (1) is multiplied by a kinematically admissible virtual displacement field  $\delta \mathbf{u}$  and integrated over the body as follows

$$\int_L \delta \mathbf{u}^T (\partial^T \mathbf{s} - \partial_b^T \mathbf{s}_b) dx = 0 \quad (3)$$

First, the section forces are written in the incremental forms  $\mathbf{s} = \mathbf{s}^0 + \Delta \mathbf{s}$  and  $\mathbf{s}_b = \mathbf{s}_b^0 + \Delta \mathbf{s}_b$ . Second, the force–deformation relations are linearized, thus  $\Delta \mathbf{s} = \mathbf{k}^0 \Delta \mathbf{e}$  and  $\Delta \mathbf{s}_b = \mathbf{k}_b^0 \Delta \mathbf{e}_b$ , in which  $\mathbf{k}^0$  and  $\mathbf{k}_b^0$  are the section initial stiffness matrices of the main body and the interface, respectively. Last, compatibility is imposed by enforcing (2). Eq. (3) then becomes

$$\int_L \delta \mathbf{u}^T \{ \partial^T (\mathbf{s}^0 + \mathbf{k}^0 \partial \Delta \mathbf{u}) - \partial_b^T (\mathbf{s}_b^0 + \mathbf{k}_b^0 \partial_b \Delta \mathbf{u}) \} dx = 0 \quad (4)$$

Eq. (4) requires integration by parts, which yields the following equation, expressed in matrix form

$$\int_L \begin{Bmatrix} \partial(\delta \mathbf{u}) \\ \partial_b(\delta \mathbf{u}) \end{Bmatrix}^T \begin{bmatrix} \mathbf{k}^0 & \mathbf{0} \\ \mathbf{0} & \mathbf{k}_b^0 \end{bmatrix} \begin{Bmatrix} \partial(\Delta \mathbf{u}) \\ \partial_b(\Delta \mathbf{u}) \end{Bmatrix} dx = [\text{Boundary Terms}] - \int_L \partial(\delta \mathbf{u})^T \mathbf{s}^0 dx \quad (5)$$

$$- \int_L \partial_b(\delta \mathbf{u})^T \mathbf{s}_b^0 dx$$

Eq. (5) expresses the integral form of equilibrium and

is the basis for the displacement-based FE formulation of the deformable bodies of Fig. 1 and Fig. 2.

In a displacement-based FE formulation, the displacements  $\mathbf{u}(x)$  along the element are approximated in terms of the nodal displacements  $\mathbf{U}$  using displacement shape functions  $\mathbf{N}_U(x)$  as follows

$$\mathbf{u} = \mathbf{N}_U \mathbf{U} \quad (6)$$

Upon substitution of (6) into (7), elimination of  $\delta \mathbf{U}$  from arbitrariness considerations and p accounting for the external virtual work  $\delta \mathbf{U}^T \mathbf{P}$ , which derives from the boundary terms in (5), the following relation results

$$\int_L \left\{ \begin{matrix} \mathbf{B} \\ \mathbf{B}_b \end{matrix} \right\}^T \begin{bmatrix} \mathbf{k}^0 & \mathbf{0} \\ \mathbf{0} & \mathbf{k}_b^0 \end{bmatrix} \left\{ \begin{matrix} \mathbf{B} \\ \mathbf{B}_b \end{matrix} \right\} dx \Delta \mathbf{U} = \mathbf{P} - \int_L \mathbf{B}^T \mathbf{s}^0 dx - \int_L \mathbf{B}_b^T \mathbf{s}_b^0 dx \quad (7)$$

where  $\mathbf{B} = \partial \mathbf{N}_U$  and  $\mathbf{B}_b = \partial_b \mathbf{N}_U$ . Eq. (7), which represents the discretized form of the governing equations, can be written as

$$\mathbf{K}^0 \Delta \mathbf{U} = \mathbf{P} - \mathbf{Q}^0 \quad (8)$$

where  $\mathbf{K}^0 = \mathbf{K}_B^0 + \mathbf{K}_b^0$  is the element stiffness matrix.  $\mathbf{K}_B^0$  is the main body contribution and  $\mathbf{K}_b^0$  is the bond contribution, defined as follows

$$\mathbf{K}_B^0 = \int_L \mathbf{B}^T \mathbf{k}^0 \mathbf{B} dx \quad \mathbf{K}_b^0 = \int_L \mathbf{B}_b^T \mathbf{k}_b^0 \mathbf{B}_b dx \quad (9)$$

$\mathbf{Q}^0 = \mathbf{Q}_B^0 + \mathbf{Q}_b^0$  are the element forces, where  $\mathbf{Q}_B^0$  is the main body contribution and  $\mathbf{Q}_b^0$  is the bond contribution, defined as

$$\mathbf{Q}_B^0 = \int_L \mathbf{B}^T \mathbf{s}^0 dx \quad \mathbf{Q}_b^0 = \int_L \mathbf{B}_b^T \mathbf{s}_b^0 dx \quad (10)$$

The selection of the interpolation functions depends on the particular element at hand and is discussed in the Applications section.

### 3.2. Force-based element

The force-based formulation for one-dimensional elements has seen a rapid development in recent years. The force-based formulation is particularly attractive for beams, because the equilibrium conditions are always satisfied point-wise along the element, irrespective of the material behavior of the section. The bending moment is linear and the axial load constant, thus 'exact' force interpolations functions can be selected. If element loads are present, the interpolation functions are easily extended. Difficulties arise when the element is inserted in a general-purpose FE program.

A fully consistent element iterative procedure is pro-

posed by Spacone et al. [3] to find the element forces corresponding to the nodal displacements. Neunhofer and Filippou [5], Petrangeli and Ciampi [4] and Petrangeli et al. [6] later simplified the algorithm by showing that a first approximation of the element forces can be obtained without element iterations, and that nodal equilibrium eventually leads to satisfaction of the element equations. The extension of the force-based formulation to the bar elements with bond-slip of Fig. 1 was accomplished by Monti et al. [7], but this formulation leads to a non-symmetric stiffness matrix. Salari et al. [8] proposed a force-based formulation for the composite beam of Fig. 2, but the element is not completely general, because it fails to converge when bond fails and the bond-slip law softens. The shortcomings in force-based approaches described above are avoided in the formulation presented here.

In a force-based FE formulation, the element is typically developed without rigid body modes, because the element flexibility matrix is eventually inverted to yield the element stiffness. In order to simplify the notation, the following derivation bears no distinction between element with and without rigid body modes, since simple transformations relate the two systems when a small displacement theory is followed.

The first step in the formulation enforces the compatibility conditions of the element. Eq. (2) are multiplied by statically admissible virtual force fields  $\delta \mathbf{s}$  and  $\delta \mathbf{s}_b$ , respectively, and the product is integrated over the body as follows

$$\int_L \delta \mathbf{s}^T (\mathbf{e} - \partial \mathbf{u}) dx + \int_L \delta \mathbf{s}_b^T (\mathbf{e}_b - \partial_b \mathbf{u}) dx = 0 \quad (11)$$

The section deformations  $\mathbf{e}$  and  $\mathbf{e}_b$  are substituted using the linearized force-deformation relations  $\mathbf{e} = \mathbf{e}^0 + \mathbf{f}^0 \Delta \mathbf{s}$  and  $\mathbf{e}_b = \mathbf{e}_b^0 + \mathbf{f}_b^0 \Delta \mathbf{s}_b$ , respectively

$$\int_L \delta \mathbf{s}^T (\mathbf{e}^0 + \mathbf{f}^0 \Delta \mathbf{s} - \partial \mathbf{u}) dx + \int_L \delta \mathbf{s}_b^T (\mathbf{e}_b^0 + \mathbf{f}_b^0 \Delta \mathbf{s}_b - \partial_b \mathbf{u}) dx = 0 \quad (12)$$

where  $\mathbf{f}^0$  and  $\mathbf{f}_b^0$  are the initial section flexibility matrices of the main body and the interface, respectively. By performing integration by parts and by applying the equilibrium conditions in (1), Eq. (12) reduces to the following equation, expressed in matrix form

$$\int_L \left\{ \begin{matrix} \delta \mathbf{s} \\ \delta \mathbf{s}_b \end{matrix} \right\}^T \begin{bmatrix} \mathbf{f}^0 & \mathbf{0} \\ \mathbf{0} & \mathbf{f}_b^0 \end{bmatrix} \left\{ \begin{matrix} \Delta \mathbf{s} \\ \Delta \mathbf{s}_b \end{matrix} \right\} dx = [\text{Boundary Terms}] - \int_L \left\{ \begin{matrix} \delta \mathbf{s} \\ \delta \mathbf{s}_b \end{matrix} \right\}^T \left\{ \begin{matrix} \mathbf{e}^0 \\ \mathbf{e}_b^0 \end{matrix} \right\} dx \quad (13)$$

In the force-based element, the internal forces of the main body,  $\mathbf{s}$ , and the interface forces,  $\mathbf{s}_b$ , are interp-

olated in terms of the element nodal forces  $\mathbf{Q}$  and the interface forces  $\mathbf{Q}_b$  at selected reference points along the interface. The resulting expression is

$$\begin{Bmatrix} \mathbf{s} \\ \mathbf{s}_b \end{Bmatrix} = \begin{bmatrix} \mathbf{N}_{BB} & \mathbf{N}_{Bb} \\ \mathbf{N}_{bB} & \mathbf{N}_{bb} \end{bmatrix} \begin{Bmatrix} \mathbf{Q} \\ \mathbf{Q}_b \end{Bmatrix} \quad (14)$$

where  $\mathbf{N}_{BB}$ ,  $\mathbf{N}_{Bb}$ ,  $\mathbf{N}_{bB}$ , and  $\mathbf{N}_{bb}$  are the force interpolation functions. Subscript B refers to the main body, and 'b' refers to the bond. In (14), it is assumed that no element loads are applied and the internal forces are functions of the nodal forces and of the reference interface forces alone. If the element is subjected to element loads, their contribution is easily added to (14) through equilibrium.

Next, (14) is expressed in incremental form (the shape functions do not change because they are based on equilibrium) and substituted into (13). By considering the virtual work done by the virtual nodal loads under the nodal displacements  $\mathbf{U}$ , and after eliminating the nodal virtual forces for arbitrariness arguments, the following expression is obtained

$$\begin{bmatrix} \mathbf{F}_{BB}^0 & \mathbf{F}_{Bb}^0 \\ \mathbf{F}_{bB}^0 & \mathbf{F}_{bb}^0 \end{bmatrix} \begin{Bmatrix} \Delta \mathbf{Q} \\ \Delta \mathbf{Q}_b \end{Bmatrix} = \begin{Bmatrix} \mathbf{U} \\ \mathbf{0} \end{Bmatrix} - \int_L \begin{bmatrix} \mathbf{N}_{BB} & \mathbf{N}_{Bb} \\ \mathbf{N}_{bB} & \mathbf{N}_{bb} \end{bmatrix}^T \begin{Bmatrix} \mathbf{e}^0 \\ \mathbf{e}_b^0 \end{Bmatrix} dx \quad (15)$$

where

$$\begin{aligned} \mathbf{F}_{BB}^0 &= \int_L (\mathbf{N}_{BB}^T \mathbf{f}^0 \mathbf{N}_{BB} + \mathbf{N}_{bB}^T \mathbf{f}_b^0 \mathbf{N}_{bB}) dx \\ \mathbf{F}_{Bb}^0 &= (\mathbf{F}_{bB}^0)^T \\ \mathbf{F}_{Bb}^0 &= \int_L (\mathbf{N}_{BB}^T \mathbf{f}^0 \mathbf{N}_{Bb} + \mathbf{N}_{bB}^T \mathbf{f}_b^0 \mathbf{N}_{bb}) dx \\ \mathbf{F}_{bb}^0 &= \int_L (\mathbf{N}_{bB}^T \mathbf{f}^0 \mathbf{N}_{bb} + \mathbf{N}_{bb}^T \mathbf{f}_b^0 \mathbf{N}_{bb}) dx \end{aligned} \quad (16)$$

The reference interface forces  $\Delta \mathbf{Q}_b$  are obtained through static condensation of (15). From the second equation

$$\Delta \mathbf{Q}_b = -(\mathbf{F}_{bb}^0)^{-1} \{ \mathbf{F}_{bB}^0 \Delta \mathbf{Q} + \tilde{\mathbf{U}} \} \quad (17)$$

where

$$\tilde{\mathbf{U}} = \int_L (\mathbf{N}_{Bb}^T \mathbf{e}^0 + \mathbf{N}_{bb}^T \mathbf{e}_b^0) dx \quad (18)$$

The bond forces  $\mathbf{Q}_b$  can be interpreted as the redundant forces of the problem, which are found by imposing compatibility of the element displacements. By substituting (17) into the first row of (15), the governing matrix equation of the element is obtained

$$\mathbf{F}^0 \Delta \mathbf{Q} = \mathbf{U} - \mathbf{U}_B^0 - \mathbf{U}_b^0 \quad (19)$$

where  $\mathbf{F}$  is the element flexibility, given by

$$\mathbf{F}^0 = \mathbf{F}_{BB}^0 - \mathbf{F}_{Bb}^0 (\mathbf{F}_{bb}^0)^{-1} \mathbf{F}_{bB}^0 \quad (20)$$

$\mathbf{U}_B^0$  and  $\mathbf{U}_b^0$  are the contributions of the main body and the interface deformations to the nodal displacements, respectively

$$\mathbf{U}_B^0 = \int_L \{ \mathbf{N}_{BB}^T - \mathbf{F}_{Bb}^0 (\mathbf{F}_{bb}^0)^{-1} \mathbf{N}_{bB}^T \} \mathbf{e}^0 dx \quad (21)$$

$$\mathbf{U}_b^0 = \int_L \{ \mathbf{N}_{bB}^T - \mathbf{F}_{bB}^0 (\mathbf{F}_{bb}^0)^{-1} \mathbf{N}_{bb}^T \} \mathbf{e}_b^0 dx$$

In order to use the present formulation in a general-purpose displacement-based FE analysis code, the flexibility matrix  $\mathbf{F}$  must be inverted to obtain the element stiffness matrix. After inversion, the rigid body modes are added using simple transformation matrices.

#### 4. Element force recovery

The element force recovery, i.e. the computation of the element resisting forces corresponding to the element displacements, requires a special procedure in force-based elements and is discussed in detail in this section. For reference purposes, the element force recovery procedure for displacement-based elements is quickly revisited first. The element force recovery procedures for both formulations are summarized in Table 2.

##### 4.1. Displacement-based element

The force recovery for this element is straightforward. The section deformations are obtained from the element displacements via the displacement interpolation functions. The corresponding section forces and stiffness are found from the section model. The element stiffness matrix  $\mathbf{K}$  is then assembled from  $\mathbf{K} = \mathbf{K}_B + \mathbf{K}_b$ , with  $\mathbf{K}_B$  and  $\mathbf{K}_b$  defined in (9) and the element forces are computed from  $\mathbf{Q} = \mathbf{Q}_B + \mathbf{Q}_b$ , with  $\mathbf{Q}_B$  and  $\mathbf{Q}_b$  defined in (10).

##### 4.2. Force-based element

Computing the element resisting forces in force-based elements is not as straightforward as in displacement-based elements. The main reason is that the displacement interpolation functions used in Eq. (10) are not available in force-based elements. Thus, the section deformations cannot be obtained from the nodal displacements, and the element forces cannot be computed from the section forces. Following early works by Mahasuverachai and Powell [9] and Zeris and Mahin [10], Spacone et al. [3] proposed an element iterative procedure that yields the element forces based on residual, or incompatible, displacements. A simplified version of the procedure was introduced by Petrangeli and Ciampi [4] and by Neuen-

Table 2

Element state determination of displacement-based and force-based one-dimensional finite elements with bond-slip ( $A_b = -(F_{bb})^{-1}F_{bB}$ )

Step	Displacement-based algorithm	Force-based algorithm
Element force increment		$\Delta Q = K^0 \Delta U$ $\Delta Q_b = A_b^0 \Delta Q - (F_{bb}^0)^{-1} \bar{U}$
Section forces		$\Delta s = N_{bb} \Delta Q + N_{Bb} \Delta Q_b$ $s = s^0 + \Delta s$ $\Delta s_b = N_{bB} \Delta Q + N_{bb} \Delta Q_b$ $s_b = s_b^0 + \Delta s_b$
Section deformations	$e = BU$ $e_b = B_b U$	$e = e^0 + f^0 \Delta s$ $e_b = e_b^0 + f_b^0 \Delta s_b$
Section state determination	$k = k(e)$ $s_R = s_R(e)$ $k_b = k_b(e)$ $s_{bR} = s_{bR}(e)$	$f = f(e)$ $s_R = s_R(e)$ $f_b = f_b(e)$ $s_{bR} = s_{bR}(e)$
Section residual deformations		$e_r = f(s - s_R)$ $e_{br} = f_b(s_b - s_{bR})$
Element stiffness	$K = \int_L B^T k B dx$ $+ \int_L B_b^T k_b B_b dx$	$F = F_{BB} - F_{Bb} (F_{bb})^{-1} F_{bB}$ $K = F^{-1}$
Element residual deformations		$U_r = \int_L \{ N_{BB} - F_{Bb} (F_{bb})^{-1} N_{bB}^T \} e_r dx$ $+ \int_L \{ N_{bB}^T - F_{Bb} (F_{bb})^{-1} N_{bb} \} e_{br} dx$
Element forces	$Q = \int_L B^T s_R dx + \int_L B_b^T s_{bR} dx$	$Q = Q^0 + \Delta Q - KU_r$ $Q_b = Q_b^0 + \Delta Q_b - A_b KU_r$
Section forces		$s = s - [N_{BB} + N_{Bb} A_b] KU_r$ $s_b = s_b - [N_{bB} + N_{bb} A_b] KU_r$
Section deformations		$e = e + e_r - f [N_{BB} + N_{Bb} A_b] KU_r$ $e_b = e_b + e_{br} - f_b [N_{bB} + N_{bb} A_b] KU_r$

hofer and Filippou [5]. The force-based formulation was applied by Monti et al. [7] to a bar element with bond-slip. The procedure is extended here to the general case of line elements with bond-slip.

The steps followed in the force recovery of force-based elements are schematically illustrated in Fig. 3. The force recovery consists of an iterative procedure at the element level based on the constraint that the element nodal displacements  $U$  remain constant while the element forces and the section deformations and forces are adjusted. Convergence is reached when the element

compatibility is satisfied in an integral sense, that is when the integral of the section deformations of (21) is equal to the element nodal displacements  $U$ , or, in other words, until the right-hand side of (19) goes to zero. In the current application, the tangent stiffness and flexibility matrices are used, thus the method corresponds to Newton–Raphson iterations under constant displacements  $U$ . The procedure applies to softening materials and softening members too, because it is carried out under imposed displacements and force peak points are easily passed (Spacone et al. [3], Petrangeli [11]). The formulation presented in this paper fully extends the force-based approach to elements with bond-slip.

The procedure is reviewed here for a single iteration at the nodal degrees of freedom (structural iteration) and is discussed for the general case of a beam element (Fig. 3). Its extension to the beam element with bond-slip contains some additional steps that regard bond, but the overall scheme remains identical and is summarized in Table 2. The problem at hand is to determine the element forces  $Q^i$  at the current global load step  $i$ , when the element displacements are incremented from those at the

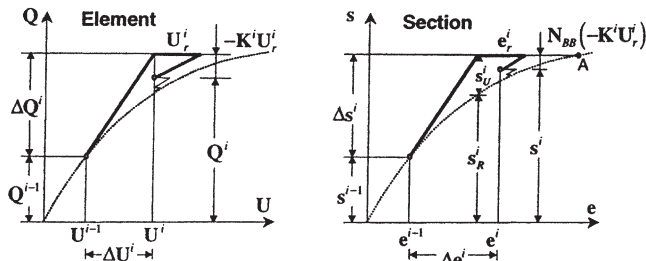


Fig. 3. Element force recovery procedure for force-based elements.

previous step  $\mathbf{U}^{i-1}$  to the current values  $\mathbf{U}^i = \mathbf{U}^{i-1} + \Delta\mathbf{U}^i$ . First, the linearized element force increment is computed using the last stiffness, that is  $\Delta\mathbf{Q}^i = \mathbf{K}^{i-1}\Delta\mathbf{U}^i$ . Using the force interpolation functions, the section force increments are computed as  $\Delta\mathbf{s}^i = \mathbf{N}_{BB}\Delta\mathbf{Q}^i$ . The section forces are updated to  $\mathbf{s}^i = \mathbf{s}^{i-1} + \Delta\mathbf{s}^i$ .

The new section deformations  $\mathbf{e}^i$  corresponding to  $\mathbf{s}^i$  must be computed. The most direct solution computes the deformations of point A in Fig. 3, but two problems arise: (1) most constitutive laws are defined in the strain or deformation space, that is the stresses are computed from the strains; (2) the procedure fails for softening constitutive laws, such as those used for concrete and for bond slip in the present paper. An alternative procedure approximates the section deformations by consistent linearization of the section constitutive law. This is accomplished by computing the section deformation increments from the last section flexibility as  $\Delta\mathbf{e}^i = \mathbf{f}^{i-1}\Delta\mathbf{s}^i$ . The section resisting forces  $\mathbf{s}_R^i$  and the new section stiffness matrix  $\mathbf{k}$  can be computed from the total section deformations  $\mathbf{e}^i = \mathbf{e}^{i-1} + \Delta\mathbf{e}^i$ . Section equilibrium is however violated, because the applied forces  $\mathbf{s}^i = \mathbf{s}^{i-1} + \Delta\mathbf{s}^i$  and the resisting forces  $\mathbf{s}_R^i$  are not identical. The unbalance force vector  $\mathbf{s}_U^i = \mathbf{s}^i - \mathbf{s}_R^i$  is transformed into a residual deformation vector  $\mathbf{e}_r^i = \mathbf{f}^i\mathbf{s}_U^i$ . Using the force interpolation functions, the element residual displacement vector is computed as  $\mathbf{U}_r^i = \int_L \mathbf{N}_{BB}^T \mathbf{e}_r^i dx$ . The residual displacements  $\mathbf{U}_r^i$  are incompatible with the element displacements  $\mathbf{U}^i$ , thus a corrective force vector  $-\mathbf{K}^i\mathbf{U}_r^i$  is applied to the element. Correspondingly, the section forces change by  $\mathbf{N}_{BB}(-\mathbf{K}^i\mathbf{U}_r^i)$  and the section deformations by  $\mathbf{f}^i\mathbf{N}_{BB}(-\mathbf{K}^i\mathbf{U}_r^i)$ . The final value of the element forces is  $\mathbf{Q}^i = \mathbf{Q}^{i-1} + \mathbf{K}^{i-1}\Delta\mathbf{U}^i - \mathbf{K}^i\mathbf{U}_r^i$ , that of the section forces  $\mathbf{s}^i = \mathbf{s}^{i-1} + \mathbf{N}_{BB}(\mathbf{K}^{i-1}\Delta\mathbf{U}^i - \mathbf{K}^i\mathbf{U}_r^i)$ , and that of the section deformations  $\mathbf{e}^i = \mathbf{e}^{i-1} + \mathbf{f}^{i-1}(\mathbf{N}_{BB}\mathbf{K}^{i-1}\Delta\mathbf{U}^i) + \mathbf{e}_r^i - \mathbf{f}^i(\mathbf{N}_{BB}\mathbf{K}^i\mathbf{U}_r^i)$  (Fig. 3).

At this point two procedures are available. Spacone et al. [3] continue the iterations until perfect convergence is reached, i.e. until the section residuals disappear (the iterations are indicated by the thin lines in Fig. 3). Petrangeli and Ciampi [4] and Neunhofer and Filippou [5] suggest to stop the procedure after the first iteration (end of the thick line in Fig. 3): structural equilibrium eventually guarantees convergence of the element incompatible displacements to zero. The first procedure is more precise and yields faster global convergence. It is however computationally more demanding at the element level. It should also be noted that convergence is faster than what schematically indicated in Fig. 3, unless very large load steps are used. The second procedure is computationally less demanding at the element level, but does not guarantee quadratic convergence of the Newton–Raphson iterations at the structural level. In both procedures, when equilibrium is reached at the nodal degrees of freedom: (1) element equilibrium is sat-

isfied in an exact form (through the force interpolation functions); (2) compatibility is satisfied in an average sense (the weighted integral of the section deformations is equal to the element displacements); (3) the section constitutive laws is satisfied exactly (i.e. within the prescribed tolerance).

The above force recovery procedure and the summary in Fig. 3 refer to the general case of a nonlinear beam element. The one-step force recovery procedure presented here and illustrated in Fig. 3 is very similar to that proposed by Neunhofer and Filippou [5], with a difference in the updating of the section deformations due to the section residual deformations. The authors prefer the proposed procedure because it guarantees element compatibility even in cases where nodal convergence is not reached, as may be the case in some intermediate load steps in a nonlinear static or dynamic frame analysis.

For the case of a beam with perfect bond, the above force-based formulation leads to the ‘exact’ solution of both the Euler–Bernoulli and the Timoshenko beam problems. When compared with displacement-based elements, force-based elements lead to a drastic reduction of the global number of degrees of freedom, since a single element can be used for each structural member in a frame analysis. This is of particular importance in the application of static and dynamic nonlinear analyses to seismic analysis and design of buildings, as outlined in new seismic design guidelines of FEMA 273 [12].

For the case of beam elements with bond slip, the formulation does not lead to the exact problem solution, since the bond fields along the element are not exactly known. The force recovery procedure for these elements is summarized in Table 2. The performance of the proposed force-based elements for this case is discussed in the next section.

## 5. Applications

Two applications are presented here to illustrate the performance of the above element formulations. The first is the problem of a reinforcing bar with bond-slip embedded in concrete (Fig. 1). The second is the problem of a steel–concrete composite beam with partial interaction between steel beam and concrete slab (Fig. 2).

In both applications, uniaxial constitutive laws are used to derive the section responses. The material laws are schematically illustrated in Fig. 4. For the bar element with bond slip, the steel bar follows the Menegotto–Pinto [13] law. The Elgehausen et al. [14] law is used for the bond-slip. For the composite beam, the fiber section model is used to derive the response of the steel beam and of the concrete slab sections. The fiber section

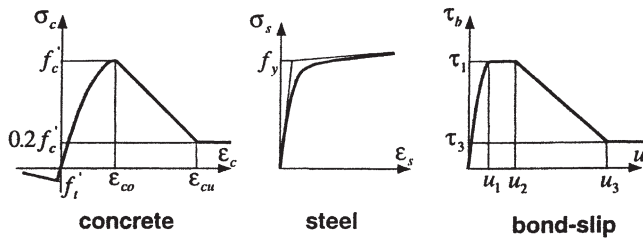


Fig. 4. Uniaxial constitutive laws.

model is discussed in Spacone et al. [3]. The steel and bond-slip constitutive laws are those used for the steel rebar with bond-slip, while the concrete uniaxial law follows the Kent and Park [15] model, modified to include the tension response of the concrete. It should be noted that tension in the concrete does not play a very important role in steel–concrete composite beams, where the concrete slab is mostly under compression. Finally, even though Fig. 4 shows only the monotonic envelopes of the constitutive laws and the following applications discuss only examples with monotonic loads, the element formulation and the material laws extend to cyclic loads, as discussed in Salari [16].

### 5.1. Reinforcing bar element with bond-slip

A two-node force-based element is illustrated in Fig. 5. The element has a quadratic bond distribution and, from equilibrium, a cubic axial load distribution in the reinforcing steel bar. The explicit values of the force interpolation functions are omitted here for the sake of the conciseness. The main reason for developing this force-based bar element was to enhance the original two-node force-based element developed by Monti et al. [7], where the formulation leads to a non-symmetric stiffness matrix. The original element by Monti et al. [7] has been inserted in a fiber element with bond-slip in the steel rebars [17], but the repeated use of a non-symmetric stiffness increases the computational effort of the element force recovery procedure.

Two numerical examples are reported. Both examples

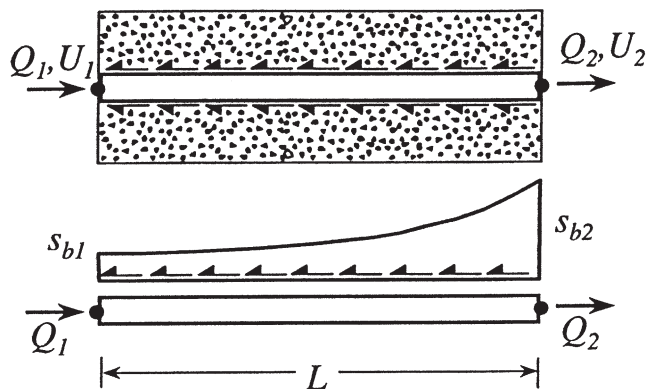


Fig. 5. 2-node force-based reinforcing bar element.

compare the experimental results obtained by Viwathanatepa et al. [18] with those obtained with the proposed element. Five Gauss–Lobatto integration points were used for both examples. The first example is the pull-out test of an anchored bar, the second one is the push-pull test of the same bar, this time loaded up to bond failure. In both examples, a #8 (24.5 mm diameter) reinforcing bar is considered. The rebar is embedded in a concrete block for 25 bar diameters (612.5 mm). In the numerical studies the concrete block is assumed perfectly rigid. The effect of the pullout cone, which has been observed in the experiments, is considered in the bond-slip law [19]. Along the confined anchorage zone of the bar, the bond material parameters corresponding to the bond-slip law of Fig. 4 are:  $\tau_1=14.85$  MPa,  $\tau_3=6.6$  MPa,  $u_1=1.0$  mm,  $u_2=3.0$  mm, and  $u_3=10.5$  mm. For the unconfined cover zone, which is assumed to extend for a length equal to four bar diameters at both ends of the bar, the bond material parameters are:  $\tau_1=8.0$  MPa,  $\tau_3=2.5$  MPa,  $u_1=0.5$  mm,  $u_2=3.0$  mm, and  $u_3=10.5$  mm. The yield stress and the initial stiffness of the reinforcing bar are  $f_y=468.5$  MPa and  $E_0=2.05 \times 10^5$  MPa, respectively. A hardening ratio of 0.014 is considered in the steel.

The results of the first test using six elements are shown in Fig. 6. The bar is pulled at the right-end only. Very good agreement is observed between the experimental and the analytical results. The change in slope in the stress-slip response of Fig. 6 at a steel stress of approximately 500 MPa corresponds to first yielding of the steel rebar. Bond reaches its maximum strength  $\tau$  at the unconfined bar end, but overall pullout of the bar is not observed because of sufficient embedment length.

The second case considers the same bar, this time pulled at the right-end and pushed at the left-end. The analytical response was obtained with six elements and is superposed to the experimental result in Fig. 7. The first major change in the response stiffness is due to yielding of the steel rebar. As the applied end displacement

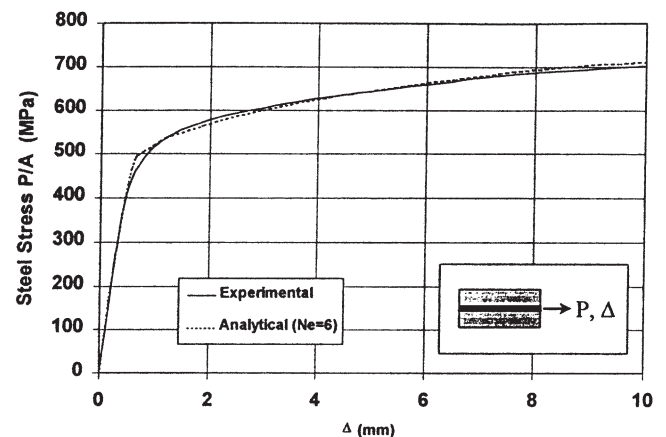


Fig. 6. Monotonic pull-out test of anchored bar (experimental data from Viwathanatepa et al. [18]).

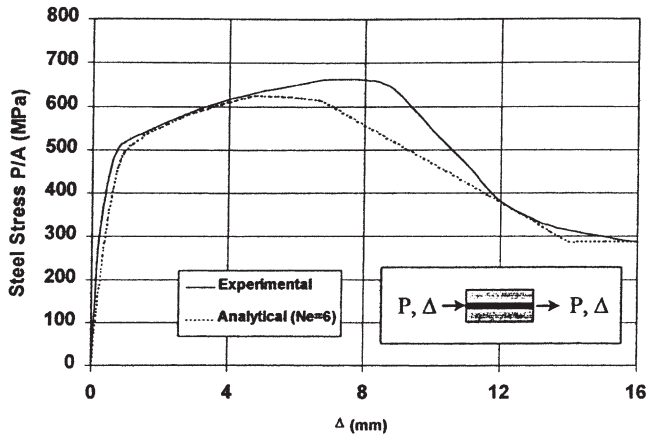


Fig. 7. Monotonic push-pull test of anchored bar (experimental data from Viwathanatepa et al. [18]).

ments are increased, bond gradually fails until the entire bar starts pulling out. No convergence problems were observed during this or other problems involving softening of the bond-slip response. Though generally very good, the overall match between experimental and analytical results could be improved, particularly in the descending branch of the response, by changing the parameters of the bond law. However, the authors preferred to use the same values in both the pull-out and in the push-pull test to show the inherent scatter in the material characteristics of the specimens. It is also worth noting that if constant bond characteristics are used throughout the specimen, only three force-based bar elements are sufficient to obtain accurate results. As for the displacement-based element, Ayoub and Filippou [19] have shown that the three-node displacement-based element, when applied to the same tests, exhibit numerical instabilities (especially when the bar response starts softening) unless a large number of elements is used.

5.2. Steel–concrete composite beam element

The two-node force-based steel–concrete composite element used in this study is shown in Fig. 8. The element has a cubic bond stress distribution. The choice of this approximation stemmed from the consideration that most tests on composite beams were performed on simply supported beams with a midspan load. In this case a parabolic bond distribution is not sufficient to accurately describe the actual bond distribution, thus a larger number of elements must be used. Cubic bond stress interpolation functions yield a more precise bond stress approximation. The force interpolation functions for this element are given by Salari [16].

For comparison purposes, a three-node displacement-based element is used in this study. The displacement-based element was first proposed by Amadio and Fragiacommo [20] and by Daniel and Crisinel [21]. The middle node of the element has only two horizontal degrees of

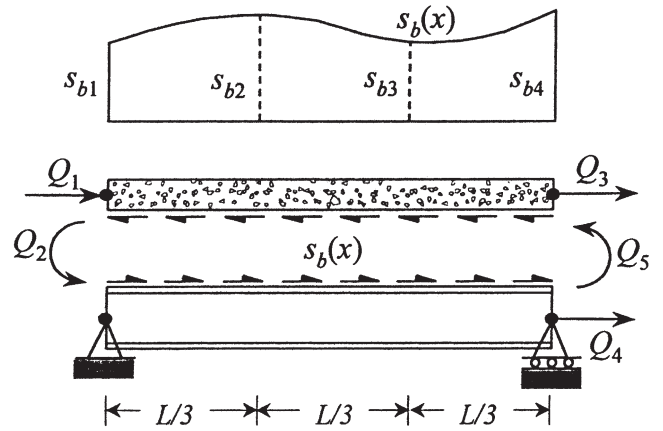


Fig. 8. 2-node force based element with cubic bond force along the beam.

freedom, one for the concrete slab and one for the steel beam. The element has a cubic shape function for the transverse displacement and a parabolic shape function for the axial displacement.

Several correlation studies with available experimental tests are presented in Salari [16], most of them on simply supported beams. For this study, a continuous two-span composite beam is used, because of the additional complexity presented by the continuity over the middle support. The beam is schematically shown in Fig. 9. The beam was tested under concentrated loads at the two mid-spans and reached an ultimate load of  $P_u=148$  kN as reported by Yam and Chapman [22]. The complete load–displacement response is not provided by Yam and Chapman [22]. The concrete compressive strength is  $f'_c=47.6$  MPa and the corresponding strain is  $\epsilon_{co}=0.0025$ . The yield stress and the modulus of elasticity for the steel girder are  $f_y=296.5$  MPa and  $E_s=2.04 \times 10^5$  MPa, respectively. A steel hardening ratio of 0.005 is considered. The shear connection between the concrete slab and the steel girder is provided along

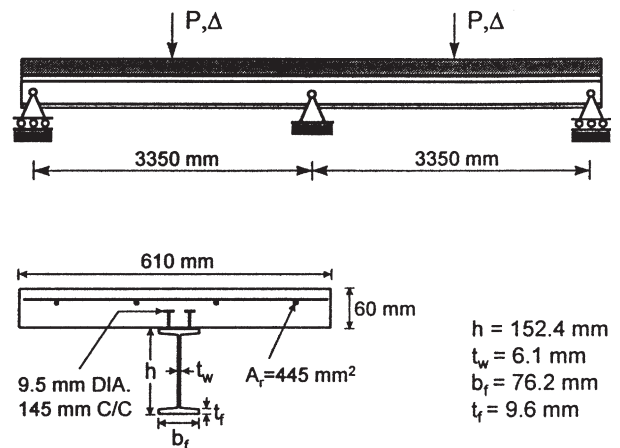


Fig. 9. Continuous steel–concrete composite beam tested by Yam and Chapman [22].

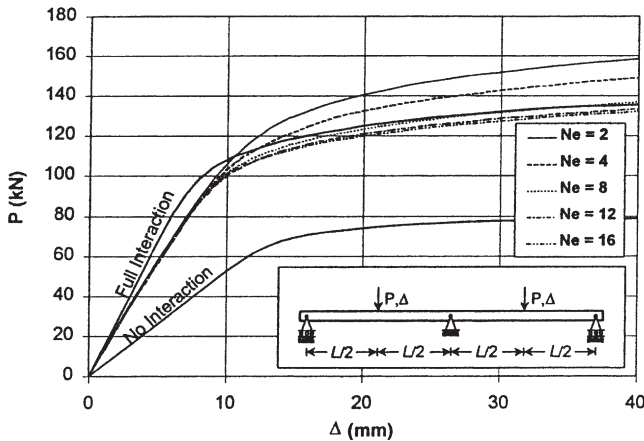


Fig. 10. Load-deflection diagrams for continuous beam: displacement-based element.

the beam by a total number of 92 headed shear studs with 9.5 mm diameter. A uniformly distributed shear capacity of  $\tau_1=440$  N/mm with the corresponding slip of  $u_1=2.25$  mm is used in the first example.

Due to symmetry, only half of the beam is analyzed. The load-deflection diagrams of the beam obtained with the displacement-based element and with the force-based element are shown in Figs. 10 and 11, respectively. The figures also contain the 'exact' solution for the same beam with full interaction (no bond-slip) and with no interaction (no bond force). Convergence is much slower with the displacement-based elements. It takes eight to twelve elements for the response to stabilize, while two force-based elements suffice to reach a satisfactory solution. The exact analytical bond force distributions along the beam at different levels of mid-span deflection are shown in Fig. 12. This solution was obtained using over fifty displacement-based elements. The bond force distribution obtained with four force-based elements per span is presented in Fig. 13. The agreement between the two distributions is quite good. It is worth pointing out the

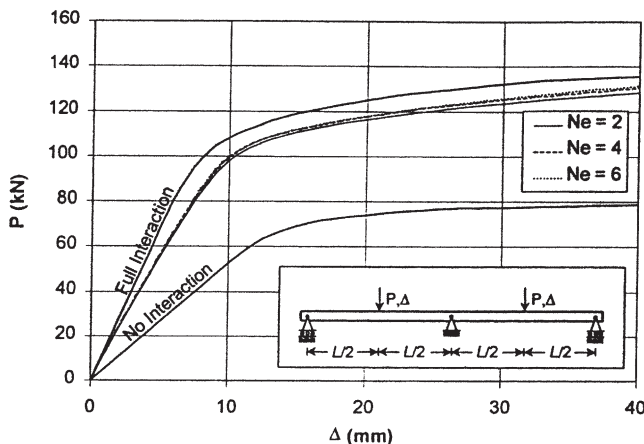


Fig. 11. Load-deflection diagrams for continuous beam: force-based element.

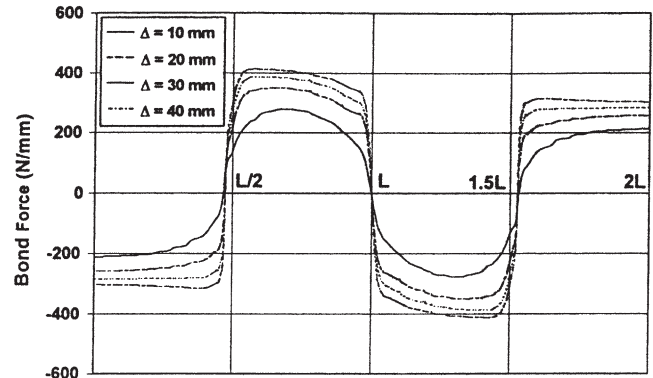


Fig. 12. Exact analytical bond force distribution along the beam.

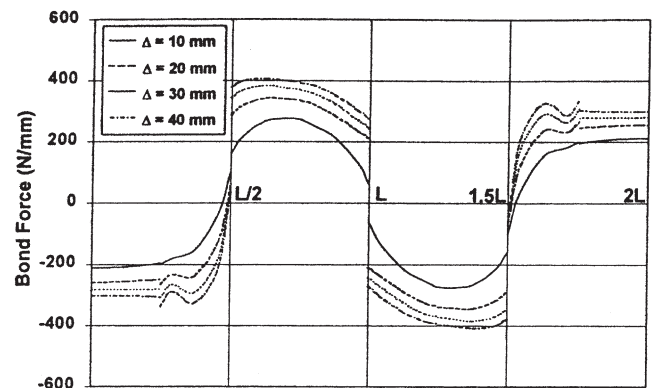


Fig. 13. Bond force distribution along the beam: force-based element.

jump, or discontinuity, in the bond-force between elements. This is consistent with the force-based formulation, where bond force continuity is not enforced at the nodes. It is also interesting to note how in the exact analytical solution the bond force is not zero under the applied load, but closer to the simple supports, because of the effect of the statically indeterminate forces. This phenomenon is only partly captured in Fig. 13, where the bond is not zero under the applied load, but changes sign in the first element between the applied load and the simple support. The average value of the bond force under the applied load (computed as the average between the bond forces in two adjacent elements) corresponds to the positive bond value of the exact solution of Fig. 12. Finally, the cubic bond interpolation functions are easily read from the bond distribution in the first element between the applied load and the simple support. In spite of this oscillation, the overall load-deflection response of Fig. 11 does not lose stability.

Finally, the same beam was used to show the element capability to describe not only concrete crushing and softening, but also softening in the bond-slip law caused by bond failure, for which the original formulation by Salari et al. [8] failed to converge. For this purpose, the beam of Fig. 9 was re-analyzed using a weaker bond with the following properties, that refer to Fig. 3:  $\tau_1=300$

N/mm,  $u_1=2.25$  mm,  $u_2=3$  mm,  $\tau_3=100$  N/mm,  $u_3=10$  mm. The beam response, obtained with four force-based elements per span, is shown in Fig. 14. The response is almost linear elastic initially, followed by a strain hardening region caused by yielding of the steel beam, up to a tip displacement of approximately 60 mm. At this point, bond reaches its capacity  $\tau_1$ , and starts softening. The effect on the force–displacement response is also a global softening. It is interesting to note that for larger imposed displacements the response does not converge to the response of the beam with no interaction (shown in Fig. 11) but to a larger force of approximately 120 kN. This is due to the residual bond strength that remains in the bond even after bond failure, as prescribed by the final region of the bond-slip response with  $\tau_3=100$  N/mm.

## 6. Conclusions

The main scope of this paper is to present the general formulation of force-based line elements (beams and bars) with bond-slip and to compare it to the classical displacement-based formulation. Existing force-based formulations for line elements with bond-slip are not totally consistent and lead to non-symmetric tangent operators, or cannot describe the complete spectrum of material behaviors, including failure and subsequent softening in the bond-slip law. The proposed force-based formulation is totally general and circumvents the above shortcomings. In order to implement the force-based element in a general-purpose FE program, a special force recovery procedure is followed. This procedure is an extension of previous formulations of force-based reinforced concrete elements with perfect bond.

Starting from the problem differential equations, the incremental forms of the displacement-based and of the force-based formulations were derived. An element force

recovery procedure based on residual (or incompatible) element displacements was presented. Two alternatives were discussed, one that relies on element iterations that lead to satisfaction of all the formulation fundamental equations, the second one without element iterations, computationally more efficient at the element level but more demanding at the structural level.

The formulation was presented in a general framework and applies to any line element with bond slip. Two applications were presented: one to a steel reinforcing bar with bond-slip embedded in a rigid concrete medium, the second to a steel beam–concrete slab composite beam with partial interaction due to flexibility of the shear studs. Both applications show the precision and reliability of the proposed force-based formulation. Even though the applications cover only monotonic loading cases, the formulation is totally general and applies also to cyclic loads.

The proposed force-based formulation applies to the case of any line element where bond-slip plays an important role and needs to be explicitly considered. The development of such elements is fundamental toward the development of rational frame elements and their use in nonlinear frame analyses. Such elements are of great theoretical and practical use, as indicated by new seismic design guidelines that require nonlinear static and dynamic analyses of building systems for assessing their performance under the design ground motions.

## Acknowledgements

This work is supported by the National Science Foundation under Grant No. CMS-9520282. This support is gratefully acknowledged. The opinions expressed in this paper are those of the authors and do not necessarily reflect those of the sponsor. The authors would also like to thank Professors P.B. Shing and D. Frangopol of the University of Colorado for their valuable insight in the early stages of the research.

## References

- [1] Carol I, Murcia J. Nonlinear time-dependent analysis of planar frames using an exact formulation. Part I: theory. Part II: computer implementation for R.C. structures. *Comput Struct* 1989;33(1):79–87, 89–102.
- [2] Molins C, Roca P. Capacity of masonry arches and spatial frames. *J Struct Eng ASCE* 1998;124(6):653–63.
- [3] Spacone E, Filippou FC, Taucer FF. Fiber beam–column model for nonlinear analysis of R/C frames. I: formulation, II: applications. *Earthq Engng Struct Dynam* 1996;25(7)(Part I):711–25 (Part II):726–42.
- [4] Petrangeli M, Ciampi V. Equilibrium based numerical solutions for nonlinear beam problem. *Int J Numer Meth Engng* 1997;40(3):423–38.

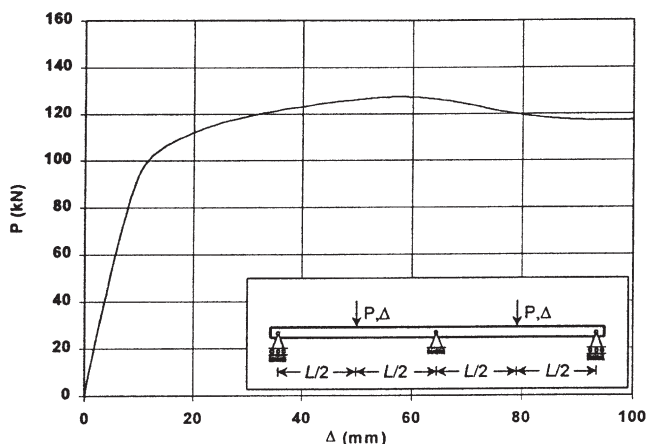


Fig. 14. Load–deflection diagrams for continuous beam with bond failure.

- [5] Neuenhofer A, Filippou F. Evaluation of nonlinear frame finite-element models. *J Struct Engng ASCE* 1997;123(7):958–66.
- [6] Petrangeli M, Pinto PE, Ciampi V. Fibre element for cyclic bending and shear for RC structures. I: theory *J Engng Mech ASCE* 1999;125(9):994–1001.
- [7] Monti G, Filippou FC, Spacone E. Finite element for anchored bars under cyclic load reversals. *J Struct Engng ASCE* 1997;123(5):614–23.
- [8] Salari MR, Spacone E, Shing PB, Frangopol DM. Nonlinear analysis of composite beams with deformable shear connectors. *ASCE J Struct Engng* 1998;124(10):1148–58.
- [9] Mahasuverachai M, Powell GH. Inelastic analysis of piping and tubular structures. EERC report 82/27, Earthquake Engineering Research Center, University of California, Berkeley, 1982.
- [10] Zeris CA, Mahin SA. Behavior of reinforced concrete structures subjected to biaxial excitation. *J Struct Engng ASCE* 1991;117(ST9):2657–73.
- [11] Petrangeli M. Fiber element for cyclic bending and shear of RC structures. II: verification *J Engng Mech ASCE* 1999;125(9):1002–9.
- [12] FEMA. NEHRP guidelines for the seismic rehabilitation of buildings. Report no. FEMA-273. Washington, DC, 1997.
- [13] Menegotto M, Pinto PE. Method of analysis for cyclically loaded reinforced concrete plane frames including changes in geometry and inelastic behavior of elements under combined normal force and bending. IABSE Symposium on Resistance and Ultimate Deformability of Structures Acted on by Well-Defined Repeated Loads, Final Report, Lisbon, 1973.
- [14] Eligehausen R, Popov EP, Bertero VV. Local bond stress–slip relationships of deformed bars under generalized excitations: experimental results and analytical model. EERC report 83–23, Earthquake Engineering Research Center, University of California, Berkeley, 1983.
- [15] Kent DC, Park R. Flexural members with confined concrete. *J Struct Div ASCE* 1971;97(ST7):1964–90.
- [16] Salari MR. Modeling of bond-slip in steel–concrete composite beams and reinforcing bars. Department of Civil, Environmental and Architectural Engineering, University of Colorado, Boulder, 1999.
- [17] Monti G, Spacone E. Reinforced concrete fiber beam element with bond-slip. *J Struct Engng ASCE* 2000;126(6):654–61.
- [18] Viathanatepa S, Popov EP, Bertero VV. Effects of generalized loadings on bond of reinforcing bars embedded in confined concrete blocks. EERC 79-22, Earthquake Engineering Research Center, University of California, Berkeley, 1979.
- [19] Ayoub A, Filippou FC. Mixed formulation of bond-slip problems under cyclic loads. *J Struct Engng ASCE* 1999;125(6):661–71.
- [20] Amadio C, Fragiaco M. A finite element model for the study of creep and shrinkage effects in composite beams with deformable shear connections. *Costruz Metall* 1993;4:213–28.
- [21] Daniel BJ, Crisinel M. Composite slab behavior and strength analysis. Part I: calculation procedure. *J Struct Engng ASCE* 1993;119(1):16–35.
- [22] Yam LCP, Chapman JC. The inelastic behavior of continuous composite beams of steel and concrete. *Proc Inst Civ Eng* 1971;2:487–501.